

Does thermal leptogenesis in a canonical seesaw rely on initial memory?

Partha Kumar Paul,^{1,*} Narendra Sahu,^{1,†} and Shashwat Sharma^{1,‡}

¹*Department of Physics, Indian Institute of Technology Hyderabad, Kandi, Sangareddy, Telangana-502285, India.*

It is a common lore that in the thermal leptogenesis in the type-1 seesaw scenario with the conventional hierarchy of heavy right-handed neutrinos (RHNs), the CP violating, out-of-equilibrium decay of the lightest RHN (N_1) is the only relevant source of $B - L$ asymmetry. Any asymmetry produced by the heavier RHNs (N_2 and N_3) gets washed out by the lepton number violating processes mediated by N_1 . In this paper, we examine this assumption comprehensively, considering decay and inverse decay processes as well as the inclusion of scatterings. We find that the above said assumption is true only if all the RHNs (N_1, N_2 and N_3) are in strong washout regime. However, we saw that, to satisfy the neutrino masses and mixing given by the low energy neutrino oscillation data, at most one of the RHNs can be in the weak washout regime. This leads to, if N_1 is in the weak washout regime, then the washout parameters of N_2 and N_3 can be chosen in such a way that the impact of N_2 and N_3 on the final $B - L$ asymmetry is relatively small. On the other hand, if N_2 or N_3 is in weak washout regime, then the asymmetry produced by them can affect the final $B - L$ asymmetry even if N_1 is in the strong washout regime, which we call the memory effect. We delineated the parameter space where the memory effect is significant.

I. INTRODUCTION

One of the most profound mysteries in cosmology is the observed baryon asymmetry of the Universe, which is the imbalance between matter and antimatter. The early Universe should have created equal amounts of matter and antimatter, but observations show that matter dominated over antimatter. This asymmetry is quantified as the baryon-to-photon ratio $\eta_B = \frac{n_B - n_{\bar{B}}}{n_\gamma} = (6.14 \pm 0.04) \times 10^{-10}$ as determined by the cosmic microwave background [1] and the big bang nucleosynthesis [2–5]. The standard model (SM) of particle physics cannot account for this observed imbalance between matter and antimatter.

Thermal leptogenesis in a canonical seesaw provides a simple yet compelling mechanism for explaining the observed baryon asymmetry of the Universe [6–12]. It connects the matter-antimatter asymmetry with the origin of non-zero neutrino mass as revealed by oscillation experiments [13–18] via the type-1 seesaw framework [19–24]. This mechanism is based on the CP violating out-of-equilibrium decay of heavy right-handed neutrinos (RHNs) to SM leptons and Higgs, producing a net lepton asymmetry which finally gets converted to the baryon asymmetry via the electroweak (EW) sphalerons [25, 26]. A common assumption in this framework is that the lightest RHN, N_1 is the primary contributor to the final $B - L$ asymmetry as any asymmetries generated by the decays of heavier RHNs (N_2, N_3) are presumed to be erased by the lepton number violating processes mediated by N_1 [11]. This assumption simplifies the analysis of thermal leptogenesis, effectively decoupling the dynamics of N_1 from N_2 and N_3 . We find that this is true only

if all the RHNs (N_1, N_2 and N_3) are in strong washout regime. However, we saw that, to satisfy the neutrino masses and mixing given by the low energy neutrino oscillation data, at most one of the RHNs can be in the weak washout regime. This leads to, if N_1 is in the weak washout regime, then the washout parameters of N_2 and N_3 can be chosen in such a way that the impact of heavier RHNs (N_2 and N_3) on the final $B - L$ asymmetry is negligible. On the other hand, if N_2 or N_3 is in weak washout regime, then the asymmetry produced by them can affect the final $B - L$ asymmetry even if N_1 is in the weak washout regime, which we call the memory effect. In this work, we study the memory effect by solving the required Boltzmann equations involving the decay, inverse decays as well as scattering processes.

Since the low energy neutrino oscillation data imply that for a given set of allowed neutrino masses and mixing only one of the RHNs can be in the weak washout regime, there can be four possibilities, i) All the RHNs are in strong washout regime, ii) Only N_1 is in weak while N_2 and N_3 are in strong washout regime, iii) Only N_2 is in the weak while N_1 and N_3 are in strong washout regime, and iv) N_3 is in the weak while N_1 and N_2 are in strong washout regime. We show that in case i, the asymmetry produced by N_2 and N_3 doesn't have any impact on the final $B - L$ asymmetry, while in the latter three cases, the $B - L$ asymmetry produced by N_2 and N_3 may play a significant role on the final $B - L$ asymmetry. In the case when N_1 is in the weak washout regime, then the asymmetry generated by $N_{2,3}$ can affect the final $B - L$ asymmetry in a certain parameter space. However, it is possible to choose the washout parameters of $N_{2,3}$ ($K_{2,3}$), and the mass hierarchy of the RHNs in such a way that the memory effect is relatively small. We also show that when N_2 is in weak washout regime¹ then the

* ph22resch11012@iith.ac.in

† nsahu@phy.iith.ac.in

‡ ph23resch11016@iith.ac.in

¹ Previous studies have explored N_2 leptogenesis scenario [27–30]

final $B - L$ asymmetry is significantly affected by N_2 generated asymmetry depending on the mass ratio of N_2 and N_1 (i.e, M_2/M_1) as well as the degree of washout by $N_{1,2}$ (i.e, $K_{1,2}$). Similarly when N_3 is in weak washout regime, the final $B - L$ asymmetry is also affected by N_3 decays depending on the mass ratio of N_3 and N_1 as well as K_1 and K_3 . A comprehensive and detailed analysis is carried out here to delineate the parameter space where the impact of N_2 and N_3 on the final $B - L$ asymmetry is significant.

The paper is organized as follows. In section II, we discuss the type-I seesaw mechanism and in section III we show the details of Boltzmann equations for leptogenesis. In Section III A we show that for a given set of low energy neutrino oscillation data, there can be only one of the RHNs in the weak washout regime. We discuss the results in section IV by comparing the percentage change (δ) in the final $B - L$ asymmetry produced by all RHNs vs only due to N_1 with respect to the mass ratios (M_2/M_1 and M_3/M_1) considering decays, inverse decays, and scatterings. We finally conclude in section V by summarizing our results and discussing the impact heavier RHNs (N_2 and N_3) on the final $B - L$ asymmetry.

II. TYPE-1 SEESAW

In the canonical type-1 seesaw, the SM is extended with three RHNs, N_1, N_2, N_3 , which are singlets under the SM gauge group ($SU(3)_C \times SU(2)_L \times U(1)_Y$). The Lagrangian responsible for generating lepton asymmetry as well as neutrino mass is given as²

$$-\mathcal{L}^{Type-1} \supset \frac{1}{2} M_R \bar{N}^c N + Y \bar{L} \tilde{H} N + H.c. \quad (1)$$

Here, $\tilde{H} = i\sigma_2 H^*$ where H is the Higgs doublet and $L = \begin{pmatrix} \nu_L \\ l_L \end{pmatrix}$ is the lepton doublet. From Eq.1 we can write the 6×6 neutral fermion mass matrix as

$$\begin{pmatrix} \bar{\nu}_L^c & \bar{N}_R \end{pmatrix} \begin{pmatrix} m_L & m_D \\ m_D^T & M_R \end{pmatrix} \begin{pmatrix} \nu_L \\ N_R^c \end{pmatrix} + H.c. \quad (2)$$

where, $m_D = \frac{Yv}{\sqrt{2}}$ (v is the Higgs vacuum expectation

value (vev)). Thus for $M_R \gg vY/\sqrt{2}$, we can write

$$m_\nu = -m_D M_R^{-1} m_D^T = -\frac{v^2}{2} Y M_R^{-1} Y^T. \quad (3)$$

Thus, the large RHN masses give an origin to the tiny masses of the active neutrinos via the type-I seesaw mechanism. The light neutrino mass matrix (m_ν) can be diagonalized using the unitary Pontecorvo–Maki–Nakagawa–Sakata (PMNS) matrix U

$$D_m = U^T m_\nu U, \quad (4)$$

where $D_m = \text{diag}(m_1, m_2, m_3)$. Using equation (3) in (4), we get

$$D_m = -\frac{v^2}{2} U^T Y M_R^{-1} Y^T U. \quad (5)$$

Let us denote $M_R = D_M = \text{diag}(M_1, M_2, M_3)$, thus from Eq.5 we can write

$$-\frac{v^2}{2} (D_{\sqrt{m^{-1}}} U^T Y D_{\sqrt{M^{-1}}}) (D_{\sqrt{m^{-1}}} Y^T U D_{\sqrt{m^{-1}}}) = I_{3 \times 3}. \quad (6)$$

Here, the notation $D_{\sqrt{A}}$ means $\sqrt{D_A}$. Since, $(D_{\sqrt{M^{-1}}} Y^T U D_{\sqrt{m^{-1}}})^T = (D_{\sqrt{m^{-1}}} U^T Y D_{\sqrt{M^{-1}}})$, we can write

$$-\frac{iv}{\sqrt{2}} (D_{\sqrt{m^{-1}}} U^T Y D_{\sqrt{M^{-1}}}) = R^T, \quad (7)$$

where, R is a complex orthogonal matrix with $R^T R = I$. Thus, using equation (7), we can write the Yukawa coupling matrix as

$$Y = \frac{i\sqrt{2}}{v} U^* D_{\sqrt{m}} R^T D_{\sqrt{M}}. \quad (8)$$

This is known as the Casas-Ibarra Parameterization of the Yukawa coupling matrix [31]. This implies that the larger values of RHNs' mass lead to larger Yukawa couplings, considering all other parameters to be fixed. The PMNS matrix U is given by [3]:

$$U = \begin{pmatrix} c_{12}c_{13} & s_{12}c_{13} & s_{13}e^{-i\delta} \\ -s_{12}c_{23} - c_{12}s_{13}s_{23}e^{i\delta} & c_{12}c_{23} - s_{12}s_{13}s_{23}e^{i\delta} & c_{13}s_{23} \\ s_{12}s_{23} - c_{12}s_{13}c_{23}e^{i\delta} & -c_{12}s_{23} - s_{12}s_{13}c_{23}e^{i\delta} & c_{13}c_{23} \end{pmatrix} \begin{pmatrix} e^{i\eta_1} & 0 & 0 \\ 0 & e^{i\eta_2} & 0 \\ 0 & 0 & 1 \end{pmatrix}, \quad (9)$$

where, $c_{ij} = \cos \theta_{ij}$ and $s_{ij} = \sin \theta_{ij}$ and δ is the Dirac CP phase and $\eta_{1,2}$ are the Majorana CP phases. For simplicity, we set the Majorana phases to be zero and take the neutrino oscillation parameters to be in the 3σ

with different approaches to demonstrate the impact of N_2 on final $B - L$ asymmetry.

² We have suppressed the generation indices.

range [32]. In the general case, the complex orthogonal

matrix R in Eq.(8) can be described by 3 different complex angles $(\theta_1, \theta_2, \theta_3)$ with a form of

$$R = \begin{pmatrix} \cos \theta_1 & -\sin \theta_1 & 0 \\ \sin \theta_1 & \cos \theta_1 & 0 \\ 0 & 0 & 1 \end{pmatrix} \begin{pmatrix} \cos \theta_2 & 0 & \sin \theta_2 \\ 0 & 1 & 0 \\ -\sin \theta_2 & 0 & \cos \theta_2 \end{pmatrix} \begin{pmatrix} 1 & 0 & 0 \\ 0 & \cos \theta_3 & -\sin \theta_3 \\ 0 & \sin \theta_3 & \cos \theta_3 \end{pmatrix} \quad (10)$$

$$= \begin{pmatrix} \cos \theta_1 \cos \theta_2 & \cos \theta_1 \sin \theta_2 \sin \theta_3 - \sin \theta_1 \cos \theta_3 & \cos \theta_1 \sin \theta_2 \cos \theta_3 + \sin \theta_1 \sin \theta_3 \\ \sin \theta_1 \cos \theta_2 & \sin \theta_1 \sin \theta_2 \sin \theta_3 + \cos \theta_1 \cos \theta_3 & \sin \theta_1 \sin \theta_2 \cos \theta_3 - \cos \theta_1 \sin \theta_3 \\ -\sin \theta_2 & \cos \theta_2 \sin \theta_3 & \cos \theta_2 \cos \theta_3 \end{pmatrix}$$

Thus given, $\theta_1, \theta_2, \theta_3, M_1, M_2, M_3$, one can derive a Yukawa coupling matrix using Eq.(8).

III. THERMAL LEPTOGENESIS IN TYPE-1 SEESAW

In the type-1 seesaw the Majorana nature of the heavy RHNs naturally leads to lepton number violation. In an expanding universe the CP violating, out of equilibrium decays of the heavy RHNs can give rise to the lepton asymmetry [6–12]. The interference between the tree-level and one-loop decay diagrams (self energy correction and vertex term) gives the required CP asymmetry, as shown in Fig. 1.

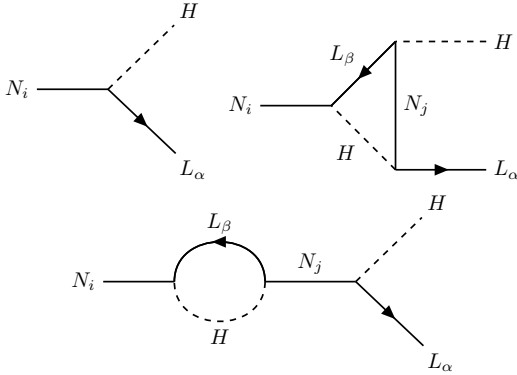


FIG. 1. Feynman diagrams for tree and one-loop level decays of RHNs giving rise to nonzero CP asymmetry.

The CP asymmetry parameter is defined as,

$$\varepsilon_i = \frac{\Gamma(N_i \rightarrow LH) - \Gamma(N_i \rightarrow \bar{L}\bar{H})}{\Gamma(N_i \rightarrow LH) + \Gamma(N_i \rightarrow \bar{L}\bar{H})} \quad (11)$$

Considering the interference of tree level diagram with one-loop diagrams we have [33]:

$$\varepsilon_i = -\frac{1}{8\pi} \sum_{j \neq i} \frac{\text{Im}[(Y^\dagger Y)_{ij}^2]}{(Y^\dagger Y)_{ii}} \left[f_v \left(\frac{M_j^2}{M_i^2} \right) + f_s \left(\frac{M_j^2}{M_i^2} \right) \right] \quad (12)$$

where, $f_v(x)$ comes from the one-loop vertex term and $f_s(x)$ comes from the one-loop self energy term and they are given by:

$$f_s(x) = \frac{\sqrt{x}}{1-x};$$

$$f_v(x) = \sqrt{x} \left[1 - (1+x) \ln \left(\frac{1+x}{x} \right) \right] \quad (13)$$

We define the comoving abundance of RHNs (N_i , for $i = 1, 2, 3$) as $N_{N_i} = n_{N_i}/n_\gamma$, where n_{N_i} is the number density of i^{th} RHN and n_γ is the photon density. Similarly we define the number density of the $B-L$ asymmetry in a comoving volume as $N_{B-L} = n_{B-L}/n_\gamma$. The Boltzmann equations (BEs) that govern the cosmological evolution of N_{B-L} and N_{N_i} are given as [11, 34, 35]

$$\begin{aligned} \frac{dN_{N_1}}{dz} &= -(D_1 + S_1)(N_{N_1} - N_{N_1}^{eq}), \\ \frac{dN_{N_2}}{dz} &= -(D_2 + S_2)(N_{N_2} - N_{N_2}^{eq}), \\ \frac{dN_{N_3}}{dz} &= -(D_3 + S_3)(N_{N_3} - N_{N_3}^{eq}), \\ \frac{dN_{B-L}}{dz} &= -\sum_{i=1}^3 [\varepsilon_i D_i(z)(N_{N_i} - N_{N_i}^{eq}) + W_i(z)N_{B-L}(z)], \end{aligned} \quad (14)$$

where $z = M_1/T$ and $D_i(z) = \frac{z\Gamma_{D_i}(\frac{M_i}{M_1}z)}{\mathcal{H}(M_i)}$ which accounts for the decays of N_i . S_i , $i = 1, 2, 3$ constitutes $\Delta L = 1$ scattering processes involving N_i . W_i represents the washout term due to inverse decays, $\Delta L = 1$ and $\Delta L = 2$ scatterings. The Hubble expansion rate is given by

$$\mathcal{H} \approx \sqrt{\frac{8\pi^3 g_*}{90}} \frac{T^2}{M_{Pl}} \approx 1.66\sqrt{g_*} \frac{T^2}{M_{Pl}}, \quad (15)$$

where, $g_* = g_{\text{SM}} = 106.75$ is the total number of degrees of freedom, $M_{Pl} = 1.22 \times 10^{19}$ GeV is the Planck mass, and T is the temperature of the thermal bath.

A. Washout Regime Analysis

Before solving the BEs 14, we define the washout parameter of N_i :

$$K_i = \frac{\Gamma_i(z = \infty)}{\mathcal{H}(z = 1)} = \frac{\tilde{m}_i M_i^2 / 8\pi v^2}{1.66\sqrt{g_*} M_i^2 / M_{Pl}} = \frac{\tilde{m}_i}{1.0697 \times 10^{-3} \text{ eV}} \quad (16)$$

where $\tilde{m}_i = \frac{v^2(Y_\nu^\dagger Y_\nu)_{ii}}{2M_i}$. If $K_i < 1$ ($\tilde{m}_i < 1.0697 \times 10^{-3}$ eV), then the i^{th} RHN is in the weak washout

regime. On the other hand, if $K_i > 1$ ($\tilde{m}_i > 1.0697 \times 10^{-3}$ eV) then the i^{th} RHN is in the strong washout regime. Using Eq.(8) we can write:

$$\begin{aligned} \tilde{m}_i &= \frac{1}{M_i} [(U^* D_{\sqrt{m}} R^T D_{\sqrt{M}})^\dagger (U^* D_{\sqrt{m}} R^T D_{\sqrt{M}})]_{ii} \\ &= \frac{1}{M_i} [(D_{\sqrt{M}} R^* D_{\sqrt{m}} U^T) (U^* D_{\sqrt{m}} R^T D_{\sqrt{M}})]_{ii} \\ &= \frac{1}{M_i} [D_{\sqrt{M}} R^* D_m R^T D_{\sqrt{M}}]_{ii} \end{aligned} \quad (17)$$

By using the generalized rotation matrix, R given by Eq.(10) and putting it in the above Eq.(17) we get:

$$\begin{aligned} \tilde{m}_1 &= |\cos \theta_1 \cos \theta_2|^2 m_1 + |\cos \theta_1 \sin \theta_2 \sin \theta_3 - \sin \theta_1 \cos \theta_3|^2 m_2 + |\cos \theta_1 \sin \theta_2 \cos \theta_3 + \sin \theta_1 \sin \theta_3|^2 m_3, \\ \tilde{m}_2 &= |\sin \theta_1 \cos \theta_2|^2 m_1 + |\sin \theta_1 \sin \theta_2 \sin \theta_3 + \cos \theta_1 \cos \theta_3|^2 m_2 + |\sin \theta_1 \sin \theta_2 \cos \theta_3 - \cos \theta_2 \cos \theta_3|^2 m_3, \\ \tilde{m}_3 &= |\sin \theta_2|^2 m_1 + |\cos \theta_2 \sin \theta_3|^2 m_2 + |\cos \theta_2 \cos \theta_3|^2 m_3, \end{aligned} \quad (18)$$

So from the above equation we notice that condition for washout regime, either $K_i < 1$ ($\tilde{m}_i < 1.0697 \times 10^{-3}$ eV) or $K_i > 1$ ($\tilde{m}_i > 1.0697 \times 10^{-3}$ eV) depends on the absolute mass of the light neutrinos which can be obtained from the neutrino oscillation data.

Now we ask the question, for a given set of light neutrino masses (m_1, m_2, m_3) how many RHNs can be in the weak washout regime ($\tilde{m}_i < 1.0697 \times 10^{-3}$ eV $\forall i$). This question can be answered from a simple analysis using the method of contradiction as given below.

For normal mass ordering (NO) of the light active neutrinos, we set $m_1 \rightarrow 0$ for simplicity, and then $m_2 = \sqrt{|\Delta m_{21}^2|}$ and $m_3 = \sqrt{\Delta m_{31}^2}$. Let us assume all RHNs to be in weak washout regime ($\tilde{m}_i < 1.0697 \times 10^{-3}$ eV $\forall i$). Now assuming $\theta_2 = \theta_3 = \frac{\pi}{2}$ in Eq.18 we get $\tilde{m}_3 \rightarrow 0$ and

$$\begin{aligned} |\cos \theta_1|^2 m_2 + |\sin \theta_1|^2 m_3 &< 1.0697 \times 10^{-3} \text{ eV}, \\ |\sin \theta_1|^2 m_2 + |\cos \theta_1|^2 m_3 &< 1.0697 \times 10^{-3} \text{ eV}. \end{aligned} \quad (19)$$

From the above inequalities, we get

$$m_2 + m_3 < 2.1394 \times 10^{-3} \text{ eV}. \quad (20)$$

Similarly in the case of inverse mass ordering (IO) of the light active neutrinos, we set $m_3 \rightarrow 0$, then $m_1 = \sqrt{|\Delta m_{31}^2|}$ and $m_2 = \sqrt{|\Delta m_{31}^2| + \Delta m_{21}^2}$. Now if we take all the RHNs to be in weak washout regime ($\tilde{m}_i < 1.0697 \times 10^{-3}$ eV $\forall i$) and $\theta_2 = \theta_3 = \frac{\pi}{2}$, we get $\tilde{m}_3 \rightarrow 0$ and

$$\begin{aligned} |\cos \theta_1|^2 m_1 + |\sin \theta_1|^2 m_2 &< 1.0697 \times 10^{-3} \text{ eV}, \\ |\sin \theta_1|^2 m_1 + |\cos \theta_1|^2 m_2 &< 1.0697 \times 10^{-3} \text{ eV}, \end{aligned} \quad (21)$$

which gives,

$$m_1 + m_2 < 2.1394 \times 10^{-3} \text{ eV}. \quad (22)$$

From Eqs.20 and 22, we see that the inequalities cannot be satisfied by the low-energy neutrino oscillation data[3, 32]. This implies that our initial assumption that all three RHNs are simultaneously in the weak washout regime is incorrect. On the other hand, from Eq.20 we can see that condition $m_2 + m_3 > 2.1394 \times 10^{-3}$ eV ($m_1 + m_2 > 2.1394 \times 10^{-3}$ eV) can be satisfied by the low-energy neutrino oscillation data for NO (IO). So the above analysis shows that when N_3 is in the weak washout regime, both N_1 and N_2 must be in the strong washout regime. This same exercise can be repeated by setting $\tilde{m}_1, \tilde{m}_2 \rightarrow 0$, which shows that for a given set of m_1, m_2, m_3 at most one of the RHNs can be in the weak washout regime[27].

Although in the above analysis we fixed the value of $\theta_2, \theta_3 = \pi/2$, it can be generalized by considering arbitrary complex values of $\theta_i \forall i$ as shown in Fig.2. For simplicity we choose the lightest neutrino mass m_1 (m_3) equal be zero for NO (IO). We illustrate the results, (i) for normal ordering in the plane of $K_3 - K_2$ with K_1 in color code as shown in Fig.2 (top) and (ii) for inverse ordering in the plane of $K_2 - K_1$ with K_3 in the color code as shown in Fig.2 (bottom). For analysis purpose, we divide Fig.2 (top) into four zones, (I) $K_2, K_3 < 1$, (II) $K_2 < 1, K_3 > 1$, (III) $K_2, K_3 > 1$ and (IV) $K_2 > 1, K_3 < 1$. In the zone (I) no points indicate that N_2 and N_3 simultaneously being in the weak washout regime is not possible. In zone (II) when N_2 is in the weak washout regime, N_1 and N_3 are in the strong washout regime. In zone (III) when N_2 and N_3 are in strong washout regime, then we have two possibilities that either N_1 is in strong washout regime (colored points) or it is in weak washout regime (black points). Finally in zone (IV) when N_3 is in the weak washout regime, then N_1 and N_2 are in strong washout regime.

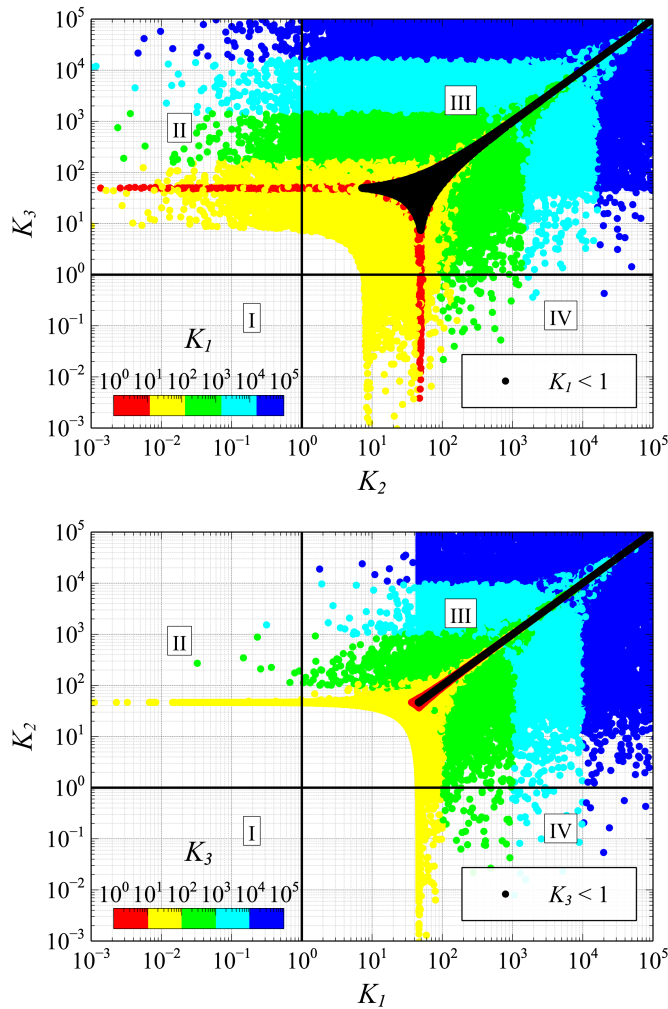


FIG. 2. Plot illustrating the constraints between K_1 , K_2 and K_3 and thereby showing that at most only one of the three *RHNs* can be in weak washout regime in the case of normal ordering (top), and inverse ordering (bottom).

The same analysis is valid for inverse ordering as shown in the Fig.2(bottom). This validates the analytical proof we showed above.

IV. DYNAMICAL EVOLUTION OF $B-L$ ASYMMETRY IN THERMAL LEPTOGENESIS

Based on the discussion in section III A, we concluded that at most one of the *RHNs* can be in a weak wash-out regime. This divides our analysis into four cases: (1) all three *RHNs* are in a strong washout regime, (2) N_1 is in a weak washout regime, (3) N_2 is in a weak washout regime, and (4) N_3 is in a weak washout regime.

As discussed in the literature [6–12], in type-1 seesaw framework, N_1 is the only d.o.f which is responsible for thermal leptogenesis. This is because, any asymmetry

produced by $N_{2,3}$ is presumed to be washed out by the lepton number violating interactions of N_1 . However, if $N_{2,3}$ is in the weak washout regime, then there is a possibility that the decay of $N_{2,3}$ can affect the $B-L$ asymmetry produced by N_1 alone. To capture this effect, we define the parameter δ as

$$\delta = \frac{N_{B-L}^{all} - N_{B-L}^1}{N_{B-L}^{all}} \times 100. \quad (23)$$

where, N_{B-L}^1 denotes the final $B-L$ asymmetry when only N_1 contribution to $B-L$ asymmetry is under consideration, and N_{B-L}^{all} denotes the final $B-L$ asymmetry when all N_1, N_2, N_3 simultaneously contribute. From Eq.23, $\delta \rightarrow 0$ implies that solving the BEs 14 considering only N_1 and considering all the *RHNs* are equivalent. In other words, $\delta \rightarrow 0$ implies N_1 is the only d.o.f, and one can neglect the contribution from $N_{2,3}$ safely. Any non-zero values of δ implies a memory effect on the final $B-L$ asymmetry. In this paper, we explore the parameter space by solving the BEs 14 for $\delta \gtrsim 15\%$.

To generate the $B-L$ asymmetry dynamically we solve the BEs.(14) considering decay, inverse decay, and scatterings involving $\Delta L = 1$, and $\Delta L = 2$ processes[36, 37]. The scattering processes considered in this analysis include:

- $\Delta L = 1$ scatterings: $NL \rightarrow \bar{Q}t$ and $Nt \rightarrow Q\bar{L}$
- $\Delta L = 2$ scatterings: $LH \rightarrow \bar{L}\bar{H}$ and $LL \rightarrow HH$

It has to be noted that scatterings are dominant in the early times, and decay dominates in later times. With these scattering processes now included, we visit all the cases mentioned above.

1. All *RHNs* are in strong washout regime

In this case, we have taken all the *RHNs* to be in the strong washout regime and varied the two mass ratios M_2/M_1 and M_3/M_1 . The top panel of Fig. 3 shows the values of δ (colored points) in the plane of M_3/M_1 and M_2/M_1 for a typical values of the washout parameters $K_1 = 101.5$, $K_2 = 122.5$, $K_3 = 166.3$. And we have also fixed the mass of N_1 to be $M_1 = 5.6 \times 10^{11} GeV$. All points in this figure correspond to the correct $B-L$ asymmetry determined by N_{B-L}^1 . We see that the change in the final $B-L$ asymmetry is negligible in this case, which validates the standard assumption in thermal leptogenesis. The strong Yukawa couplings of all *RHNs* drive rapid interactions that effectively eliminate any asymmetry produced by $N_{2,3}$, leaving N_1 as the only effective d.o.f. for the final $B-L$ asymmetry.

The bottom panel of Fig.3 illustrates a benchmark point showing the evolution of the number densities of *RHNs* N_1 (solid green), N_2 (solid red), and N_3 (solid magenta). The $B-L$ asymmetry generated by N_1

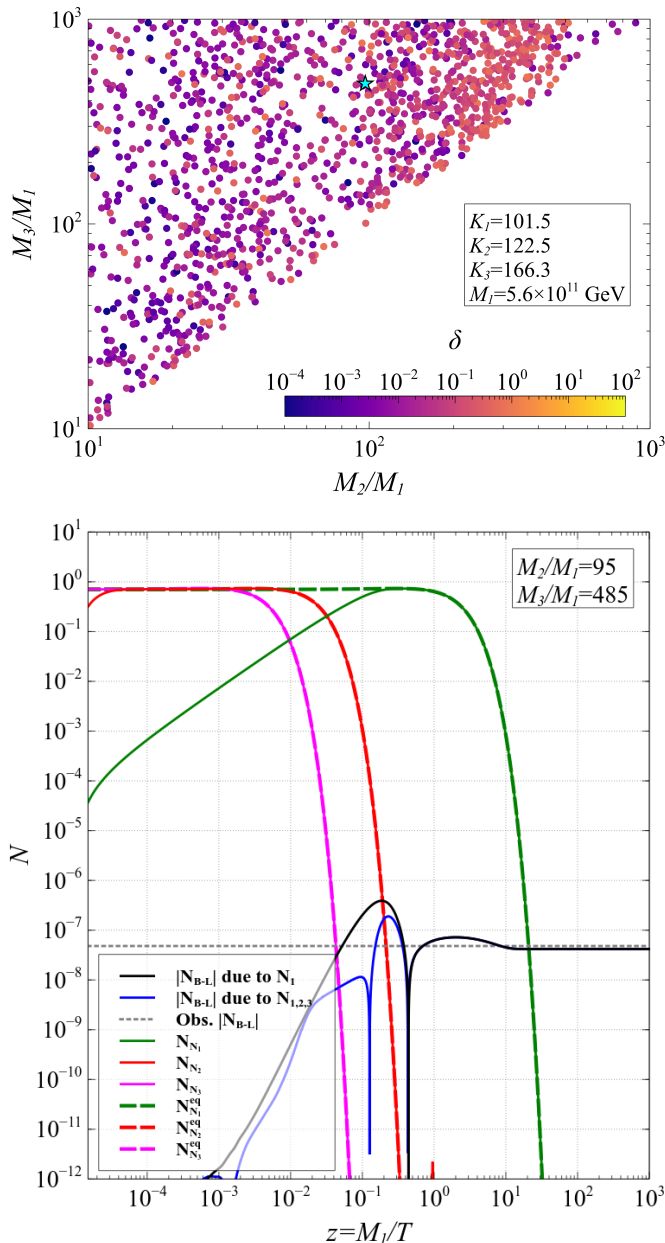


FIG. 3. (top) Allowed parameter space in the plane M_3/M_1 vs M_2/M_1 when all the RHNs are in strong washout regime. The color code depicts the δ values representing the memory effect. (bottom) Cosmological evolution of comoving number densities of RHNs and $B-L$ asymmetries for the blue star point when all RHNs are in strong washout regime

alone is shown by the solid black curve, whereas the solid blue curve represents the asymmetry produced by N_1, N_2 and N_3 all together. The chosen mass ratios, $M_2/M_1, M_3/M_1 = 95, 485$, respectively, represent a typical hierarchical structure (*i.e.* $M_3 \gg M_2 \gg M_1$). In the strong washout regime, all RHNs undergo rapid decays and scatterings, leading to an increase in their number densities and the production of asymmetries. However,

the large Yukawa couplings also result in rapid inverse decays and scatterings, which quickly wash out the generated asymmetry.

Here we see that the scatterings contribute significantly to the washout of the asymmetry at small z values, corresponding to higher temperatures in the early Universe. This enhanced washout at earlier times reduces the initial condition for N_1 . Thus the asymmetry produced by N_1 alone becomes the final $B-L$ asymmetry. This shows that in the case when all RHNs are in the strong washout regime, there is no memory effect and hence N_1 can be considered as the sole effective d.o.f. for obtaining the final $B-L$ asymmetry.

2. N_1 is in weak washout regime

Now, we consider the scenario where N_1 is in the weak washout regime. As indicated in Fig. 2, if N_1 is in the weak washout regime, then the other two RHNs, N_2 and N_3 , must necessarily be in the strong washout regime. We solve the BEs 14 with typical choice of $K_1 = 9.7 \times 10^{-3}$, $K_2 = 85.1$, $K_3 = 123.8$ along with $M_1 = 5.97 \times 10^{12}$ GeV. The resulting value of δ is shown in Fig.4 (top), in the plane of $M_3/M_1 - M_2/M_1$. All points in this figure correspond to the correct $B-L$ asymmetry determined by N_{B-L}^1 . Since N_1 is in weak washout regime, the Yukawa coupling of N_1 is very weak for decays, inverse decays and scatterings. Thus, one might expect that the pre-existing asymmetry left by N_2 and N_3 should persist in the final result and we should therefore see a large memory effect. But contrary to expectations, we see a small memory effect ($\delta \lesssim 30\%$) on the final $B-L$ asymmetry when the RHNs are hierarchical. This can be understood as follows. Since N_2 and N_3 are in a strong washout regime, their scattering processes suppress the asymmetry production from their decays at early times. As a result, the contribution of N_2 and N_3 to the final $B-L$ asymmetry is substantially reduced. In other words, the initial condition for the $B-L$ asymmetry produced by N_1 is already diminished by earlier processes. Therefore, in this case, the memory effect is relatively small. Consequently, N_1 remains as the primary degree of freedom for the final asymmetry even if N_1 is in the weak washout regime.

This behavior is illustrated with a benchmark point in Fig. 4 (bottom), where we take $M_2/M_1 = 10$ and $M_3/M_1 = 485$. The comoving number densities of N_1, N_2 and N_3 are illustrated by solid green, red and magenta respectively. The $B-L$ asymmetry produced by only N_1 is shown by the solid black curve whereas, blue curve represents the combined asymmetry produced N_1, N_2 and N_3 . The gross behavior can be understood as follows. Here, N_3 , having the largest mass, decays first and produces a small asymmetry due to large washout effects. However, this small asymmetry is quickly erased by N_2 's scattering-induced washout processes. Once N_3 has fully decayed, N_2 begins producing asymmetry be-

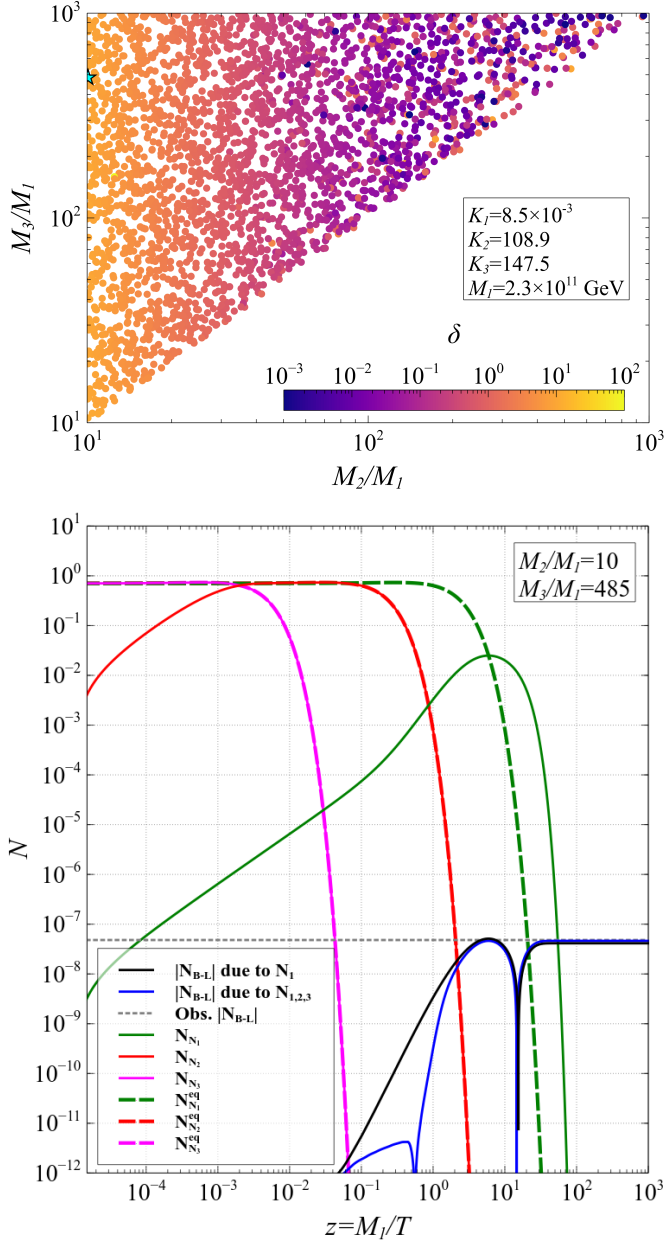


FIG. 4. (top) Allowed parameter space in the plane M_3/M_1 vs M_2/M_1 when N_1 is in weak washout regime. The color code depicts the δ values representing the memory effect. (bottom) Cosmological evolution of comoving number densities of RHNs and $B-L$ asymmetries for the blue star point when N_1 is in weak washout regime.

ing in equilibrium. Therefore, the inverse decays are not suppressed, resulting in a suppression of N_2 generated asymmetry. This leads to a minimal initial condition for N_1 generated $B-L$ asymmetry.

In Fig.4, we saw that when N_1 is in a weak washout regime, there is not much memory effect ($\delta \lesssim 30\%$) left on the final $B-L$ asymmetry. But now we give a general overview of the case when N_1 is in the weak washout

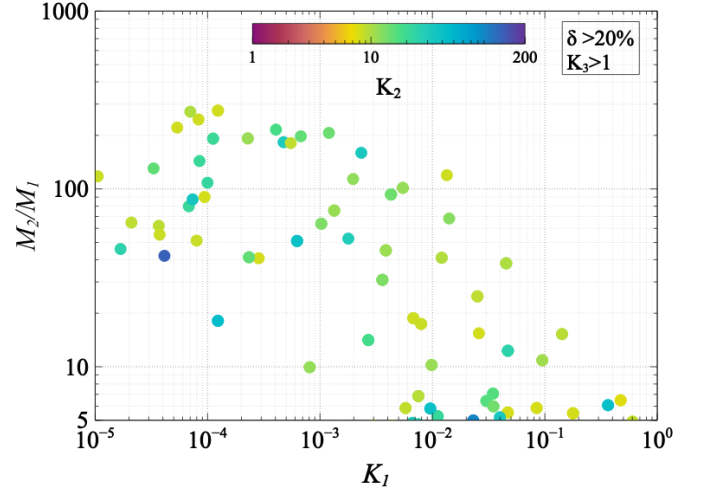


FIG. 5. A summary plot illustrating the impact of $N_{2,3}$ on final $B-L$ asymmetry when N_1 is in weak washout regime.

regime in Fig.5. In this figure, we illustrate the memory effect ($\delta > 20\%$) in the plane of K_1 vs M_2/M_1 and K_2 is in the color code with $K_3 > 1$. Here we show that unlike, Fig.4, the memory effect survives when the K_1 is small. As the K_1 increases ($K_1 \rightarrow 1$), M_2/M_1 must decrease to maintain the $\delta > 20\%$. The value of K_2 is also important as larger value of K_2 implies, stronger washout by N_2 , which erases the pre-existing asymmetry produced by $N_{2,3}$. In other words, a larger K_2 implies that the impact of $N_{2,3}$ of the final $B-L$ asymmetry is smaller. Recall that K_i doesn't depend of the RHN masses, therefore for a given choice of M_2/M_1 , we can increase the value of K_2 in order to reduce the memory effect.

3. N_2 is in weak washout regime

We now move to the case where N_2 is in the weak washout regime, while N_1 and N_3 remain in the strong washout regime. We consider a typical case by taking $K_1 = 111.9$, $K_2 = 5.5 \times 10^{-4}$, $K_3 = 151.2$ and the mass of N_1 is $M_1 = 3.7 \times 10^{12}$ GeV. Figure 6 (top) shows the variation of the values of δ in the plane of M_2/M_1 and M_3/M_1 . All points in this figure correspond to the correct $B-L$ asymmetry determined by N_{B-L}^1 .

From Fig.6 (top) we see that in a large parameter space δ takes non-zero values. Typically for $M_2/M_1 \sim 10$, $\delta > 50\%$. This is because when N_2 mass is close to N_1 , the production of $B-L$ asymmetry from the out-of-equilibrium decays of N_2 occurs after the washout effects of N_1 are suppressed. As a result N_1 doesn't get enough time to washout the asymmetry generated by N_2 even though it is in strong washout regime. On the other hand, if $M_2 \gg M_1$, then decay of N_2 happens early. As a result, the asymmetry produced by N_2 and N_3 is heavily washed out by the scatterings processes and inverse

decays mediated by N_1 leading to small δ values.

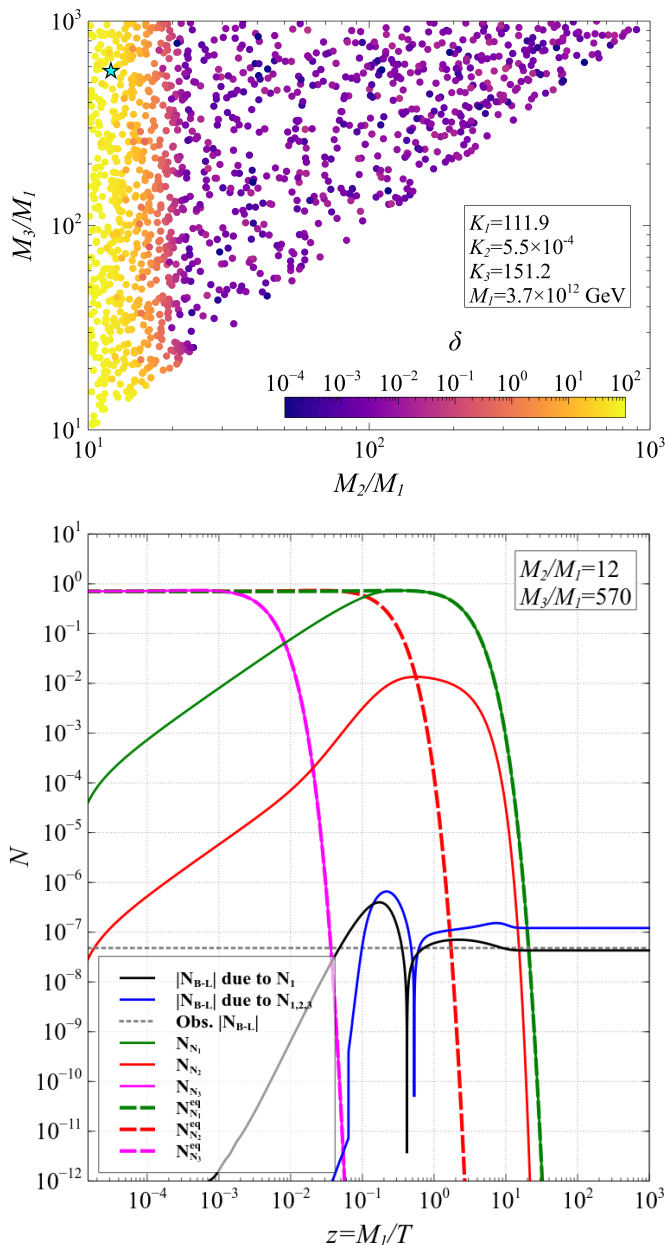


FIG. 6. (top) Allowed parameter space in the plane M_3/M_1 vs M_2/M_1 when N_2 is in weak washout regime. The color code depicts the δ values representing the memory effect. (bottom) Cosmological evolution of comoving number densities of RHNs and $B-L$ asymmetries for the blue star point when N_2 is in weak washout regime.

This scenario is further studied in detail by taking a benchmark point (shown as by a blue star mark in Fig.6 (top)), with its evolution depicted in Fig. 6 (bottom). Here, we consider $M_2/M_1 = 12$ and $M_3/M_1 = 570$. The comoving number densities of N_1 , N_2 and N_3 are illustrated by solid green, red, and magenta, respectively. The $B-L$ asymmetry produced only by N_1 is shown

by the solid black curve, whereas the blue curve represents the combined asymmetry produced by N_1 , N_2 and N_3 . Now N_2 , being in the weak washout regime, decays out of equilibrium and generates asymmetry in the vicinity of N_1 , while the washout effects of N_1 are already suppressed, resulting in large δ values.

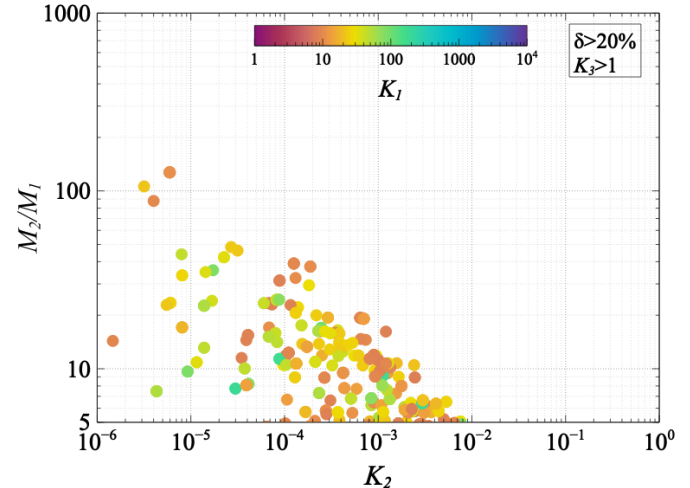


FIG. 7. A summary plot illustrating the impact of $N_{2,3}$ on the final $B-L$ asymmetry when N_2 is in the weak washout regime.

Finally, to highlight the regions where the memory effect is large ($\delta > 20\%$) in the case when N_2 is in weak washout regime, we present a scatter plot in the M_2/M_1 vs K_2 plane, with K_1 shown in the color code. As seen in Fig. 7, when K_2 increases — meaning the Yukawa coupling of N_2 becomes stronger — both M_2/M_1 and K_1 must decrease for N_2 to impact the final $B-L$ asymmetry. On the other hand, for larger M_2/M_1 , the Yukawa coupling of N_2 must decrease, therefore, K_2 becomes smaller.

4. N_3 is in weak washout regime

Now we consider the case where N_3 is in the weak washout regime and N_1 and N_2 are in the strong washout regime. We solve the BEs 14 with a typical choice of $K_1 = 155.1$, $K_2 = 119.4$, $K_3 = 3.1 \times 10^{-4}$ along with $M_1 = 2.9 \times 10^{12}$ GeV. All points in the Fig.8 correspond to the correct $B-L$ asymmetry determined by N_{B-L}^1 . One might expect that any asymmetry produced by N_3 should be washed out due to fast inverse decay and scattering interactions mediated by N_1 and N_2 . However, in Fig.8 (top), we see that there exists a small parameter space where we can get the memory effect ($\delta > 1$) in the final asymmetry. This non-zero values of δ survives only when the mass ratios satisfy $M_3/M_1 \gtrsim M_2/M_1 \lesssim 20$. At higher mass ratios, the asymmetry generated by N_3 undergoes significant suppression due to the strong washout

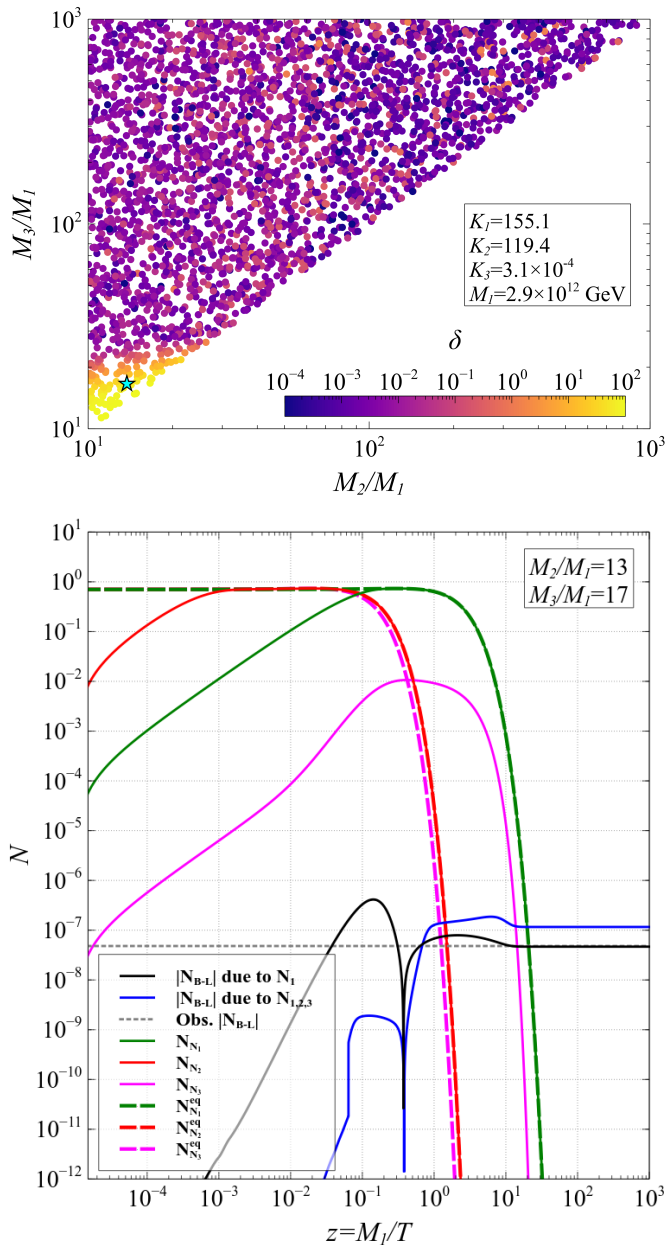


FIG. 8. (top) Allowed parameter space in the plane M_3/M_1 vs M_2/M_1 when N_3 is in weak washout regime. The color code depicts the δ values representing the memory effect. (bottom) Cosmological evolution of comoving number densities of RHNs and $B-L$ asymmetries for the blue star point when N_3 is in weak washout regime.

effects induced by both the scattering and inverse decays mediated by N_1 and N_2 .

This behavior is further explained in Fig. 8(bottom), where we consider the benchmark mass ratios $M_2/M_1 = 13$ and $M_3/M_1 = 17$, ensuring that the mass ratios are relatively close. Being in weak washout regime, N_3 decays significantly out of equilibrium, occurring well after the decay of N_2 and close to that of N_1 where the washout

effects of N_1 are already suppressed. This results in the large δ values.

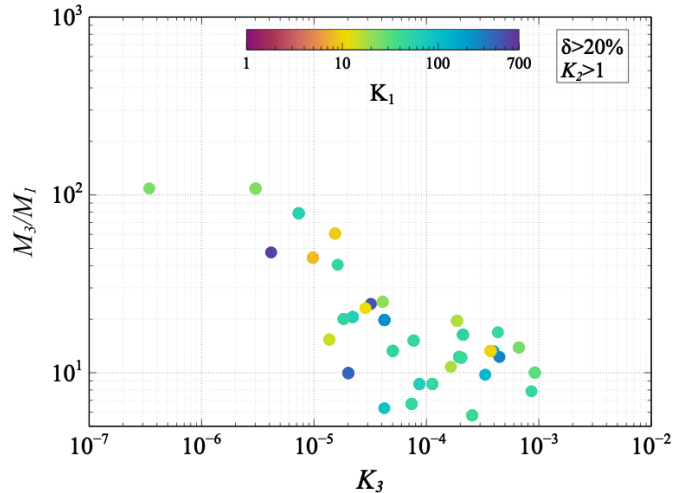


FIG. 9. A summary plot illustrating the impact of $N_{2,3}$ on the final $B-L$ asymmetry when N_3 is in the weak washout regime.

Now to summarize the case when N_3 is in weak washout regime, we illustrate the memory effect ($\delta > 20\%$) by showing a scatter plot in the plane of M_3/M_1 vs K_3 and K_1 in the color code in Fig.9. Here, we observe a similar pattern as Fig.7. That is, as K_3 increases, the mass ratio M_3/M_1 must decrease for N_3 to influence the final $B-L$ asymmetry. Now for large M_3/M_1 , the Yukawa coupling of N_3 must decrease to have an impact on the final $B-L$ asymmetry, which means that K_3 must decrease.

V. CONCLUSIONS

In thermal leptogenesis, it is assumed that only the lightest right-handed neutrino is the relevant degree of freedom in a hierarchical scenario. We have examined the validity of this assumption by explicitly solving the Boltzmann equations 14, considering i) combined $B-L$ asymmetry (N_{B-L}^{all}) generated by N_1 , N_2 and N_3 and, ii) $B-L$ asymmetry (N_{B-L}^1) generated by N_1 alone. We then define a parameter δ to measure the difference between the above mentioned scenarios. We checked that the neutrino oscillation data allow for a given set of low-energy parameters to have at most one of the right-handed neutrino in the weak washout regime. We use this condition to explore all the possible scenarios. We find that the assumption of considering N_1 as the only relevant degree of freedom is valid only when all RHNs are in the strong washout regime. When N_1 , N_2 or N_3 is in the weak washout regime, then depending on the Yukawa couplings and the mass ratios (M_2/M_1 and M_3/M_1), the asymmetry produced due to heavier neutrinos impacts

the final $B - L$ asymmetry. We found that in the case when N_1 is in the weak washout regime, then the asymmetry generated by $N_{2,3}$ can affect the final $B - L$ asymmetry in a certain parameter space. However, by choosing suitable values of K_2 and M_2/M_1 , the memory effect can be minimized. On the other hand, when N_2 is in a weak washout regime, the memory effect survives in a large parameter space. In particular, for M_2/M_1 ranging from 5 to 100 the corresponding K_2 values lie in the range 10^{-2} to 10^{-6} . A similar conclusion is also drawn when N_3 is in weak washout regime. In this case, the memory effect again survives in a large parameter space. In particular, for M_3/M_1 ranging from 5 to 100 the cor-

responding K_3 values lie in the range 10^{-3} to 10^{-6} .

ACKNOWLEDGMENTS

P.K.P. would like to acknowledge the Ministry of Education, Government of India, for providing financial support for his research via the Prime Minister's Research Fellowship (PMRF) scheme. The works of N.S. is supported by the Department of Atomic Energy - Board of Research in Nuclear Sciences, Government of India (Ref. Number: 58/14/15/2021-BRNS/37220).

-
- [1] N. Aghanim *et al.* (Planck), *Astron. Astrophys.* **641**, A6 (2020), [Erratum: *Astron.Astrophys.* 652, C4 (2021)], [arXiv:1807.06209 \[astro-ph.CO\]](#).
 - [2] B. Fields and S. Sarkar, (2004), [arXiv:astro-ph/0406663](#).
 - [3] S. Navas *et al.* (Particle Data Group), *Phys. Rev. D* **110**, 030001 (2024).
 - [4] R. H. Cyburt, B. D. Fields, K. A. Olive, and E. Skillman, *Astropart. Phys.* **23**, 313 (2005), [arXiv:astro-ph/0408033](#).
 - [5] G. Steigman, *Int. J. Mod. Phys. E* **15**, 1 (2006), [arXiv:astro-ph/0511534](#).
 - [6] M. Fukugita and T. Yanagida, *Phys. Lett. B* **174**, 45 (1986).
 - [7] M. A. Luty, *Phys. Rev. D* **45**, 455 (1992).
 - [8] R. N. Mohapatra and X. Zhang, *Phys. Rev. D* **46**, 5331 (1992).
 - [9] M. Flanz, E. A. Paschos, and U. Sarkar, *Phys. Lett. B* **345**, 248 (1995), [Erratum: *Phys.Lett.B* 384, 487–487 (1996), Erratum: *Phys.Lett.B* 382, 447–447 (1996)], [arXiv:hep-ph/9411366](#).
 - [10] S. Davidson, E. Nardi, and Y. Nir, *Phys. Rept.* **466**, 105 (2008), [arXiv:0802.2962 \[hep-ph\]](#).
 - [11] W. Buchmuller, P. Di Bari, and M. Plumacher, *Annals Phys.* **315**, 305 (2005), [arXiv:hep-ph/0401240](#).
 - [12] R. Barbieri, P. Creminelli, A. Strumia, and N. Tetradis, *Nucl. Phys. B* **575**, 61 (2000), [arXiv:hep-ph/9911315](#).
 - [13] P. F. de Salas, D. V. Forero, C. A. Ternes, M. Tortola, and J. W. F. Valle, *Phys. Lett. B* **782**, 633 (2018), [arXiv:1708.01186 \[hep-ph\]](#).
 - [14] K. Abe *et al.* (T2K), *Phys. Rev. D* **91**, 072010 (2015), [arXiv:1502.01550 \[hep-ex\]](#).
 - [15] M. G. Aartsen *et al.* (IceCube), in *34th International Cosmic Ray Conference* (2015) [arXiv:1510.05223 \[astro-ph.HE\]](#).
 - [16] J. N. Bahcall and C. Pena-Garay, *New J. Phys.* **6**, 63 (2004), [arXiv:hep-ph/0404061](#).
 - [17] S. Fukuda *et al.* (Super-Kamiokande), *Phys. Rev. Lett.* **86**, 5656 (2001), [arXiv:hep-ex/0103033](#).
 - [18] K. Eguchi *et al.* (KamLAND), *Phys. Rev. Lett.* **90**, 021802 (2003), [arXiv:hep-ex/0212021](#).
 - [19] P. Minkowski, *Phys. Lett. B* **67**, 421 (1977).
 - [20] M. Gell-Mann, P. Ramond, and R. Slansky, *Conf. Proc. C* **790927**, 315 (1979), [arXiv:1306.4669 \[hep-th\]](#).
 - [21] O. Sawada and A. Sugamoto, eds., *Proceedings: Workshop on the Unified Theories and the Baryon Number in the Universe: Tsukuba, Japan, February 13-14, 1979* (Natl.Lab.High Energy Phys., Tsukuba, Japan, 1979).
 - [22] R. N. Mohapatra and G. Senjanović, *Phys. Rev. Lett.* **44**, 912 (1980).
 - [23] J. Schechter and J. W. F. Valle, *Phys. Rev. D* **22**, 2227 (1980).
 - [24] J. W. F. Valle and J. C. Romao, *Neutrinos in high energy and astroparticle physics*, Physics textbook (Wiley-VCH, Weinheim, 2015).
 - [25] A. D. Sakharov, *Pisma Zh. Eksp. Teor. Fiz.* **5**, 32 (1967).
 - [26] V. A. Kuzmin, V. A. Rubakov, and M. E. Shaposhnikov, *Phys. Lett. B* **155**, 36 (1985).
 - [27] P. Di Bari, *Nucl. Phys. B* **727**, 318 (2005), [arXiv:hep-ph/0502082](#).
 - [28] G. Engelhard, Y. Grossman, E. Nardi, and Y. Nir, *Phys. Rev. Lett.* **99**, 081802 (2007), [arXiv:hep-ph/0612187](#).
 - [29] F. Hahn-Woernle, *JCAP* **08**, 029, [arXiv:0912.1787 \[hep-ph\]](#).
 - [30] M. Re Fiorentin, *PoS CORFU2014*, 121 (2015).
 - [31] J. A. Casas and A. Ibarra, *Nucl. Phys. B* **618**, 171 (2001), [arXiv:hep-ph/0103065](#).
 - [32] P. F. de Salas, D. V. Forero, S. Gariazzo, P. Martínez-Miravé, O. Mena, C. A. Ternes, M. Tortola, and J. W. F. Valle, *JHEP* **02**, 071, [arXiv:2006.11237 \[hep-ph\]](#).
 - [33] S. Davidson and A. Ibarra, *Phys. Lett. B* **535**, 25 (2002), [arXiv:hep-ph/0202239](#).
 - [34] W. Buchmuller, P. Di Bari, and M. Plumacher, *Nucl. Phys. B* **643**, 367 (2002), [Erratum: *Nucl.Phys.B* 793, 362 (2008)], [arXiv:hep-ph/0205349](#).
 - [35] M. Plumacher, *Z. Phys. C* **74**, 549 (1997), [arXiv:hep-ph/9604229](#).
 - [36] R. Pramanick, T. S. Ray, and A. Sil, *Phys. Rev. D* **109**, 115011 (2024), [arXiv:2401.12189 \[hep-ph\]](#).
 - [37] G. F. Giudice, A. Notari, M. Raidal, A. Riotto, and A. Strumia, *Nucl. Phys. B* **685**, 89 (2004), [arXiv:hep-ph/0310123](#).